Kinetics and Catalysis, Vol. 44, No. 5, 2003, pp. 639–647. From Kinetika i Kataliz, Vol. 44, No. 5, 2003, pp. 700–708.

CATALYTIC REACTION MECHANISMS

Elucidation of the Surprising Role of NO in N_2O Decomposition over FeZSM-5[1]

J. Pérez-Ramírez*, G. Mul, F. Kapteijn**, and J. A. Moulijn****

**Hydrocarbon Processes and Catalysis, Norsk Hydro, Research Center, P.O. Box 2560, N-3907, Porsgrunn, Norway*

***Reactor and Catalysis Engineering, Delft University of Technology, Julianalaan 136, 2628 BL, Delft, The Netherlands*

e-mail: javier.perez.ramirez@hydro.com

Received October 9, 2002

Abstract—The decomposition of N_2O is strongly promoted by NO over steam-activated FeZSM-5. The promoting effect of NO is catalytic, and in addition to NO_2, O_2 is formed much more extensively at lower temperatures than in the absence of NO. The promotion effect only requires low NO concentrations in the feed, with no significant improvements at molar NO/N_2O feed ratios higher than 0.25. No inhibition by NO was identified even at a molar NO/N_2O feed ratio of 10, suggesting different sites for NO adsorption and oxygen deposition by N_2O. The latter sites seem to be remote from each other. Transient experiments using *in situ* FT-IR/MS and Multitrack over FeZSM-5 further elucidate the mechanism of NO promotion. The release of oxygen from the catalyst surface during direct N_2O decomposition is a rate-determining step due to the slow oxygen recombination, which is favored by high reaction temperatures. NO addition promotes this oxygen desorption, acting as an oxygen transfer agent, probably via NO_2 species. Adsorbed NO may facilitate the migration of atomic oxygen to enhance their recombination. Less than 0.9% of Fe seems to participate in this promotion. A model is proposed to explain the phenomena observed in NO-assisted N_2O decomposition, including NO_2 decomposition.

INTRODUCTION

An intriguing general feature of FeZSM-5 catalysts in direct N_2O decomposition is that NO significantly enhances the activity, while the opposite effect is usually observed for other catalytic systems, e.g., based on transition (Cu, Co) and noble metals (Ru, Rh) [1–5]. This peculiar behavior of FeZSM-5 makes it very attractive to use in applications where both N_2O and NO are present, such as in tail-gas of nitric acid plants [6, 7]. The positive effect of NO on the N_2O conversion was first reported by some of us in 1996, using a FeZSM-5 prepared by ion exchange with Fe(II) sulfate [2]. At that time it was proposed that NO in the gas-phase scavenged adsorbed oxygen (deposited by N_2O during the oxidation of active sites, Eq. (I)), leading to the formation of NO_2 and regeneration of the active site (Eq. (II)) [3]:

$$N_2O + \square \longrightarrow N_2 + O\square, \quad \text{(I)}$$

$$NO + O\square \longrightarrow NO_2 + \square. \quad \text{(II)}$$

Reduction of an oxidized site by NO as represented in Eq. (II) should lead to a stoichiometric process in which NO and N_2O react to form N_2 and NO_2:

$$N_2O + NO \longrightarrow N_2 + NO_2. \quad \text{(III)}$$

Recently, Sang and Lund [8] further discussed the mechanism of NO-assisted N_2O decomposition over a FeZSM-5 catalyst prepared by sublimation. These authors proposed a nitrite/nitrate redox cycle (Eqs. (IV), (V)) by reaction with N_2O, yielding O_2 and N_2. However, no experimental evidence was provided to support this:

$$N_2O + NO_3^- \longrightarrow N_2 + O_2 + NO_2^-, \quad \text{(IV)}$$

$$N_2O + NO_2^- \longrightarrow N_2 + NO_3^-. \quad \text{(V)}$$

The present work further investigates the mechanism of NO-assisted N_2O decomposition over steam-activated FeZSM-5. Activity data on the effect of the molar NO/N_2O feed ratio and reaction temperature on the catalytic performance is presented. Based on flow and pulse experiments, in combination with *in situ* FTIR/MS, steady-state and transient phenomena regarding the chemistry of N_2O, NO, and NO_2 over FeZSM-5 are investigated, and possible catalytic cycles in NO-assisted N_2O decomposition are proposed.

EXPERIMENTAL

Isomorphously substituted FeZSM-5 was synthesized hydrothermally using TPAOH as the template [9, 10]. The molar ratios between the components were $H_2O/Si = 45$, $TPAOH/Si = 0.3$, $Si/Al = 36$, and $Si/Fe = 152$. The as-synthesized sample was calcined in air at 823 K for 10 h and converted into the H-form by three consecutive exchanges with an ammonium nitrate solution (0.1 M) for 12 h and subsequent air calcination at 823 K for 5 h. Finally, the catalyst was treated in flow-

[1] This article was submitted by the authors in English.

0023-1584/03/4405-0639$25.00

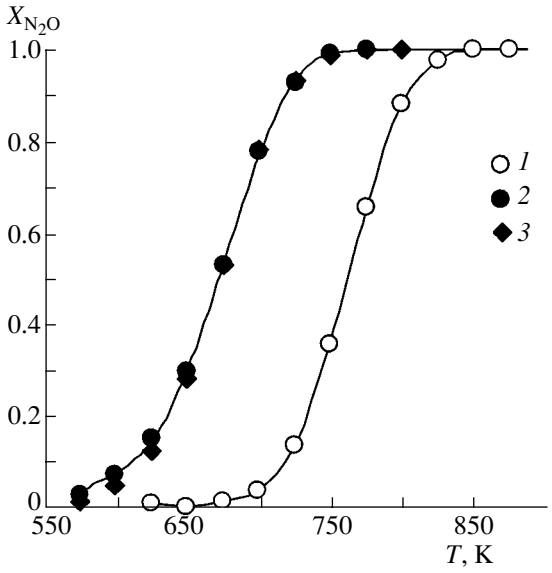

Fig. 1. N_2O (X_{N_2O}) conversion vs. temperature over ex-FeZSM-5 in different feed mixtures: (*1*) 1.5 mbar N_2O in He and (*2*) 1.5 mbar N_2O + 0.4 mbar NO in He, (*3*) 1.5 mbar N_2O + 0.4 mbar NO + 20 mbar O_2 in He; $m/v(N_2O)_0 = 8.65 \times 10^5$ g s/mol; P = 1 bar.

ing steam at ambient pressure (water partial pressure of 300 mbar and 30 ml/min of N_2 flow) at 873 K for 5 h, yielding a sample denoted as ex-FeZSM-5.

Activity measurements were carried out in a six-flow reactor system [11], using 50 mg of catalyst (125–200 μm) and a space time of 8.65×10^5 g s/mol. The space time is defined as the ratio $m/v(N_2O)_0$, where m is the catalyst mass and $v(N_2O)_0$ the molar flow of N_2O at the reactor inlet. The feed conditions used were 1.5 mbar N_2O, 0–15 mbar NO, 0–0.2 mbar NO_2, and 0–20 mbar O_2 with He as the balance gas. Before reaction, the catalysts were pretreated in 1.5 mbar N_2O in He at 723 K for 1 h and cooled in that gas flow to the initial reaction temperature. N_2O, N_2, and O_2 were analyzed with a GC equipped with a thermal conductivity detector. NO, NO_2, and NO_x concentrations were determined with a chemiluminescence NO_x analyzer.

The FT-IR (Fourier transform infrared) measurements were performed using an *in situ* infrared cell with CaF_2 windows [12]. The catalyst was pressed in the form of a self-supporting wafer (~70 mg/cm^2) at a pressure of 3 ton/cm^2. Gas flows were set by mass-flow controllers, and composition programming was carried out using a four-way valve, which was configured to select two separate gas feeds. Pretreatment of the wafer consisted of drying at 573 K in He for 1 h. Spectra were recorded using a Nicolet Magna infrared 860 spectrometer equipped with a nitrogen cooled MCT detector and a rapid scan interferometer. Transient experiments were performed at a resolution of 4 cm^{-1} and using coaddition of 48 scans. Spectra were recorded against a background of the sample at the reaction temperature under He. Scan length minimization was used, leading to a complete spectrum collection time of 7.7 s. The infrared measurements were performed using a 3 vol % N_2O in He mixture and a 5 vol % NO in He mixture (in both cases 30 ml/min). The purity of all the gases was >99.985%. The transients in gas-phase composition were followed using a quadrupole mass spectrometer (Pfeiffer Thermostar) connected on line to the outlet of the *in situ* infrared cell via a capillary.

A detailed description of the Multitrack (multiple time resolved analysis of catalytic kinetics) system is presented elsewhere [13]. Two different gases can be dosed to the reactor by means of high-speed pulse valves, yielding pulses of 10^{17} molecules within 100 μs. The reactor with the catalyst sample is located in a high vacuum system, and during pulsing the peak pressure remains below 3 Pa. The catalyst bed (100 mg, pellet size 125–200 μm) is packed between two layers of inert SiC particles. At the reactor exit, the reaction products are analyzed by a quadrupole mass spectrometer positioned in-line with the reactor axis. As the signal-to-noise ratio in this system is excellent, single pulses are sufficient to obtain good peak signals. This is an important aspect, as transient phenomena may remain unobserved when several pulse responses have to be averaged. Before the Multitrack measurements, the catalysts were evacuated *in situ* at 723 K for 3 h. The mechanistic studies of direct N_2O decomposition were carried out by continuously pulsing pure N_2O (~160 nmol per pulse) with intervals of 2 s ("cycle time") at different temperatures in the range 623–973 K and recording the masses *m/e*: 28 (N_2), 32 (O_2), and 44 (N_2O). The effect of NO on the N_2O decomposition was studied in dual-pulse experiments in which pulses of N_2O (pure, ~160 nmol per pulse) and NO (15 vol % NO in Ar, ~24 nmol NO per pulse) are sequentially fed to the reactor with a time interval of 1 s between the pulses and a cycle time of 2 s. Isothermal transient desorption effects after stopping N_2O or NO pulsing were followed at different temperatures, ranging from 698 to 923 K. In these experiments, the masses *m/e* 30 (NO) and 46 (NO_2) were additionally analyzed. The purity of the gases was >99.985%.

RESULTS

Activity experiments. The N_2O decomposition activity of ex-FeZSM-5 (Si/Al = 32.6, 0.66 wt % Fe) in different feed mixtures is presented in Fig. 1. In a N_2O/He feed, the catalysts show substantial N_2O conversion only above 700 K. The addition of NO (0.4 mbar; $NO/N_2O = 0.27$) enhances the reaction rate considerably. The N_2O conversion curve is shifted to about 100 K lower temperatures. The presence of oxygen (20 mbar O_2) in the feed (N_2O + NO + O_2 in He) hardly affects the catalyst activity. Figure 2 shows the influence of the molar NO/N_2O ratio in the feed on the N_2O conversion over ex-FeZSM-5 at reaction tempera-

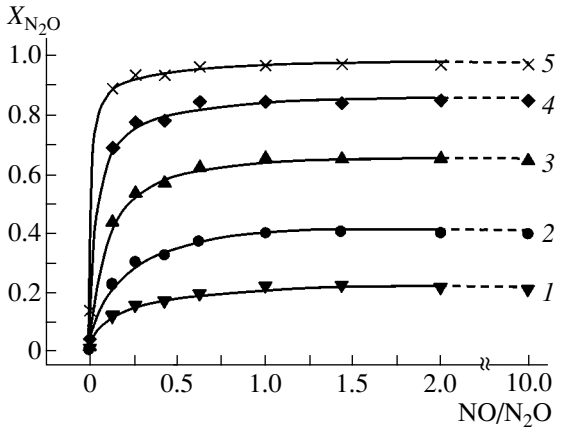

Fig. 2. N_2O (X_{N_2O}) conversion vs. the molar NO/N_2O feed ratio over ex-FeZSM-5 at different temperatures: (*1*) 623, (*2*) 648, (*3*) 673, (*4*) 698, and (*5*) 723 K. Partial N_2O pressure was fixed at 1.5 mbar and partial NO pressure varied from 0 to 15 mbar; $m/v(N_2O)_0 = 8.65 \times 10^5$ g s/mol; P = 1 bar.

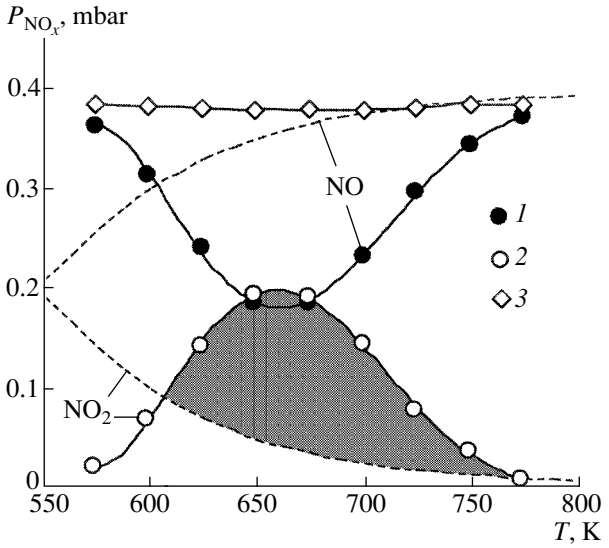

Fig. 3. Partial pressure of (*1*) NO, (*2*) NO_2, and (*3*) NO_x vs. temperature over ex-FeZSM-5. Conditions: 1.5 mbar N_2O + ~0.4 mbar NO in He; $m/v(N_2O)_0 = 8.65 \times 10^5$ g s/mol; P = 1 bar. Equilibrium composition of NO and NO_2 (Eq. (VI)) are represented by dashed lines.

tures ranging from 623 to 723 K. N_2O conversion is dramatically improved at low NO partial pressures ($NO/N_2O < 0.25$). From this value up to $NO/NO_2 = 10$, little effect on N_2O conversion is noticed.

The NO, NO_2, and NO_x profiles provide further information on the effect of NO on the catalytic performance. In a (N_2 + NO)/He feed, the formation of NO_2 over ex-FeZSM-5 increases as a function of reaction temperature (Fig. 3), reaching a maximum at 650–675 K, i.e., around the inflection point of the N_2O decomposition activity curve (Fig. 1). Above this temperature, NO_2 formation decreases before completely disappearing at 775 K. The total NO_x level is constant in the temperature range investigated, indicating that NO_x is not converted to N_2 or N_2O. The formation of NO_2 is beyond the thermodynamic equilibrium of Eq. (VI) (gray area in Fig. 3), suggesting that the reaction between N_2O and NO (Eq. (III)) proceeds faster than Eq. (VI):

$$2NO + O_2 \longleftrightarrow 2NO_2. \qquad \text{(VI)}$$

The equilibrium composition of NO_2 and NO was calculated assuming an O_2 availability corresponding with the amount if N_2O conversion would be 100% (P_{O_2} = 0.75 mbar). These theoretical partial pressure profiles of NO and NO_2 are displayed in Fig. 3 by the dashed lines. The occurrence of the N_2O and NO reaction should be attributed to the catalytic performance of ex-FeZSM-5, since no NO_2 formation was observed over an inert material (SiC) in the same feed composition (not shown).

In Fig. 4 the amount of NO_2 produced and O_2 produced is plotted vs. the amount of N_2O reacted to N_2 at 700 K for different inlet partial NO pressures. These results clearly show that the stoichiometric reaction of N_2O with NO to NO_2 and N_2 (Eq. (III)) cannot solely explain the promotion effect observed in Fig. 1. Besides inducing the formation of N_2O, the presence of NO in the NO_2-containing feed also significantly enhances the production of O_2, closing the oxygen mass balance (long dashed line *3* in Fig. 4). Further information on the relatively low amount of NO_2 formed compared to

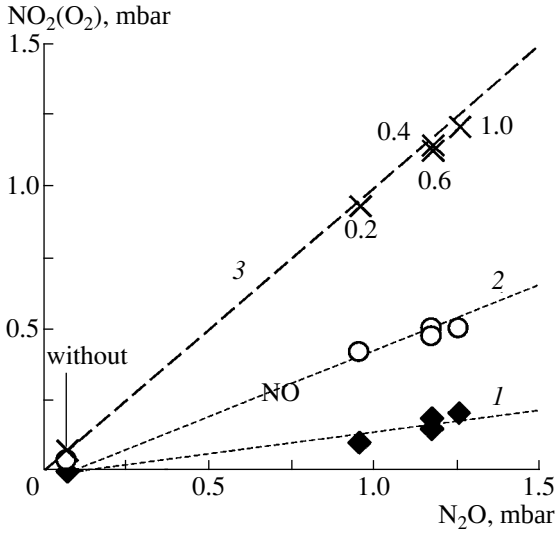

Fig. 4. NO_2 (*1*) and O_2 (*2*) formed vs. N_2O converted at 700 K over ex-FeZSM-5 at different partial NO pressures (mbar) in the feed. Crosses (×) represent the $NO_2 + O_2$ measured experimentally and the diagonal (long) dashed line the mass balance for oxygen. The numbers refer to the NO/N_2O ratio in the feed. Conditions: 1.5 mbar N_2O + (0–1 mbar NO) in He; $m/v(N_2O)_0 = 8.65 \times 10^5$ g s/mol; P = 1 bar.

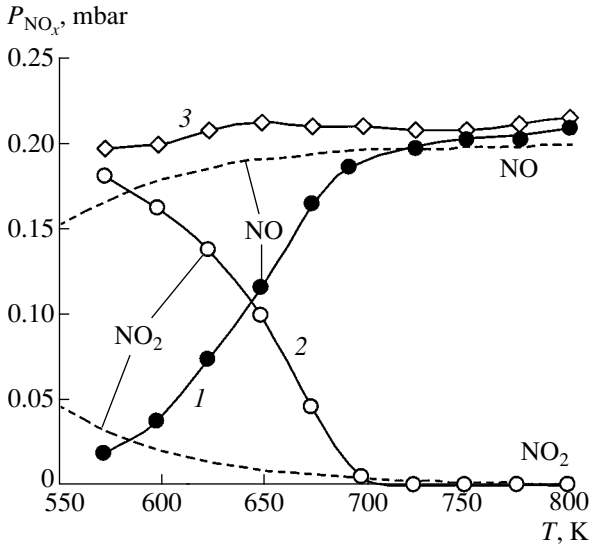

Fig. 5. Partial pressure of (*1*) NO, (*2*) NO_2, and (*3*) NO_x vs. temperature over ex-FeZSM-5. Feed composition: 0.2 mbar NO_2 in He; $m/v(N_2O)_0 = 8.65 \times 10^5$ g s/mol; $P = 1$ bar; equilibrium compositions of NO and NO_2 (Eq. (VI)) are represented by dashed lines.

the amount of N_2O decomposed can be related to the decomposition reaction of NO_2 to NO and O_2. By feeding a mixture of NO_2 in He over ex-FeZSM-5, the NO_2 decomposition rate was analyzed. The result for $P_{NO_2} = 0.2$ mbar is shown in Fig. 5. NO_2 is converted into NO and O_2 over the catalyst in the temperature range where the promotion effect of NO occurs. Equilibrium is reached above 700 K, which indicates that NO_2 decomposition and NO oxidation by NO_2 (Eq. (VI)) occur fairly fast. This result suggests that NO_2 decomposition might contribute to the formation of O_2. Production of NO is hardly observed over inert material (SiC, not shown).

***In situ* FT-IR/MS experiments.** The transients occurring when NO adsorbed on ex-FeZSM-5 is exposed to N_2O or vice versa were measured at 523 K. The gas-phase composition was changed from 5 vol % NO in He to 3 vol % N_2O in He and back to 5 vol % NO in He. Upon the introduction of N_2O in the cell at 523 K, bands assigned to gas-phase N_2O appear at around 2225 cm^{-1} in the infrared spectra presented in Fig. 6. A continuous decrease of the bands assigned to adsorbed NO can be observed. After an induction period of 30 s, a new band develops around 1632 cm^{-1}, which continuously grows in intensity and can be assigned to adsorbed NO_2 on Fe(II) [14–16]. The corresponding gas-phase product evolution at 523 K is shown in Fig. 7 (region *I*). A time delay is observed between the time of switching the gas from NO to N_2O and the formation of N_2, in agreement with the infrared observations. The formation of NO_2 was not detected at this temperature. Upon switching the gas-phase composition from N_2O back to NO, a rapid transition from the 1635 cm^{-1} to the original bands at around 1886 and 1874 cm^{-1} were observed in Fig. 8. At the same time, the MS analysis shows that NO_2 is formed immediately (Fig. 7, region *II*), as well as some N_2. The N_2 produced is related to the limited time that both NO and N_2O are present in the infrared cell.

Multitrack experiments. Multitrack was used to further investigate the formation of O_2 during N_2O decomposition and the influence of NO in the N_2O conversion over ex-FeZSM-5. A typical Multitrack profile during direct N_2O decomposition at 823 K over this catalyst after 100 pulses is presented in Fig. 9. The N_2O and N_2 signals are very similar in shape. The O_2 response signal of the N_2O pulse deviates from the N_2O and N_2 signal, being much broader. In order to discriminate if the shape of the oxygen is due to a mechanistic feature of N_2O decomposition or simply due to nonreactive adsorption–desorption phenomena of O_2 along the catalyst bed, molecular oxygen was pulsed. In this case, the pulse is very similar in shape to that of N_2 and

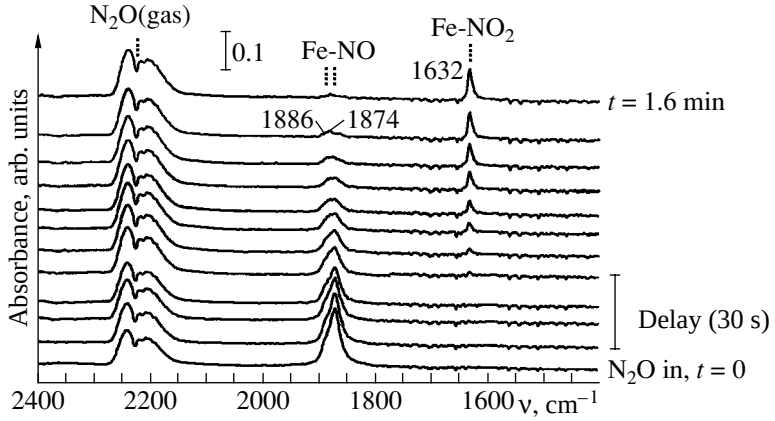

Fig. 6. Transient infrared spectra of NO adsorbed on ex-FeZSM-5 at 523 K upon switching a flow (30 ml/min) of 5 vol % NO in He to a flow (30 ml/min) of 3 vol % N_2O in He. Spectra were recorded against a background of the catalyst at 523 K in He.

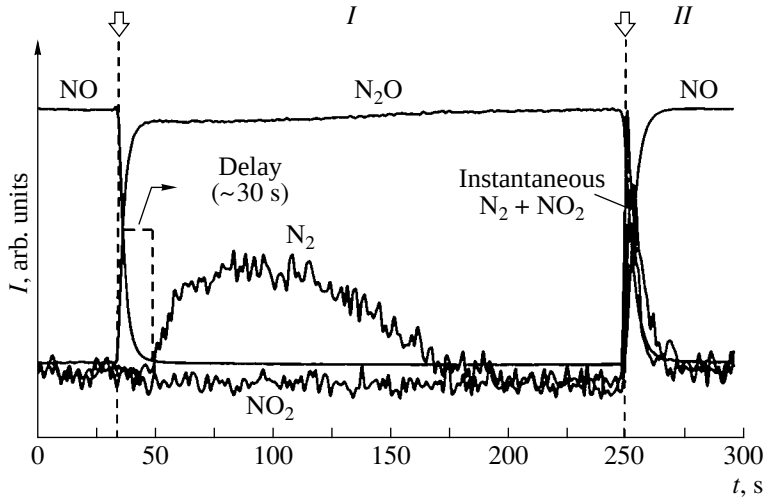

Fig. 7. Transient in gas composition upon switching a flow (30 ml/min) of 5 vol % NO in He to a flow (30 ml/min) of 3 vol % N_2O in He at $t = 0$ (region *I*) and back to a flow (30 ml/min) of 5 vol % NO in He at $t = 250$ s (region *II*).

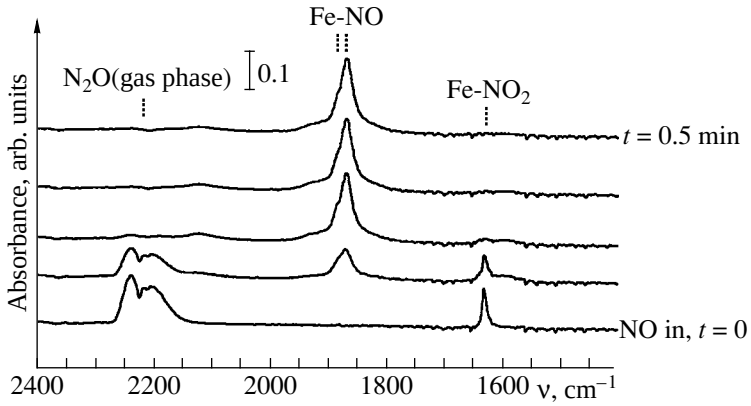

Fig. 8. Transient infrared spectra of NO_2 adsorbed on ex-FeZSM-5 at 523 K upon switching a flow (30 ml/min) of 3 vol % N_2O in He back to a flow (30 ml/min) of 5 vol % NO in He. Spectra were recorded against a background of the catalyst at 523 K in He.

N_2O (not shown), confirming the validity of the first hypothesis. The delay of the oxygen signal was further investigated by pulsing N_2O at different reaction temperatures. These results are shown in Fig. 10. In the range 573–673 K, a very broad oxygen signal is observed. At 723 K, the oxygen signal becomes more pronounced. Around 873 K, the signal significantly sharpens, indicating that the rate of desorption of oxygen from the catalyst surface is significantly enhanced.

To study the effect of NO on O_2 formation in N_2O decomposition, dual-pulse experiments were carried out at different temperatures, in which N_2O and NO were pulsed at 0.1 and 1 s, respectively, repeated in cycles of 2 s. Pulsing N_2O (at 0.1 s) over ex-FeZSM-5 at 773 K leads to broad oxygen signal (Fig. 11, profile (*1*)), indicating a relatively slow desorption of O_2. Alternate pulsing of N_2O and NO for 10 cycles leads to a remarkable effect on the O_2 response at the time of the N_2O pulse. The O_2 response sharpens (Fig. 11, profile (*2*)), indicating a significantly faster O_2 desorption in N_2O–NO cycles than in the experiment with only N_2O. Stopping NO pulsing results in a transition back to the original catalyst behavior in six cycles (12 s), with a very broad O_2 response (Fig. 11, profiles (*3*, *4*)). At lower temperatures, the promotion effect lasts longer. At 698 K, the promotion vanishes 20 cycles (40 s) after the NO pulsing is stopped. This indicates that adsorbed species formed at the time of the NO pulse are involved in the enhanced O_2 formation and their stability towards desorption determines the duration of the effect. The sharp oxygen signal is rapidly recovered after four pulses of NO (Fig. 11, profiles (*5*, *6*)).

During the dual-pulse experiments at these temperatures, no NO or NO_2 signals were observed at the time of the N_2O pulse, which indicates that NO does not block N_2O decomposition sites. NO_2 formation was observed but only at the time of the NO pulse (Fig. 11, profile (*7*)). The MS technique did not allow quantification of the NO_2 desorption. At high temperatures (e.g., 973 K), the effect of NO on the oxygen desorption

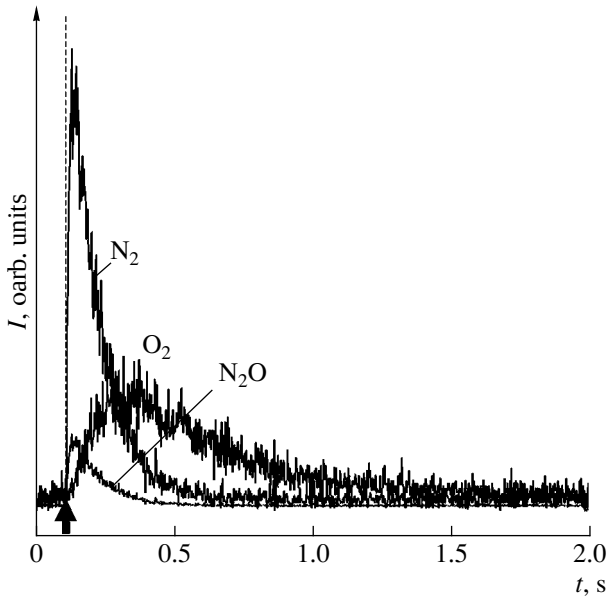

Fig. 9. Typical Multitrack profiles of N_2O, N_2, and O_2 during pulsing of pure N_2O over ex-FeZSM-5 at 823 K.

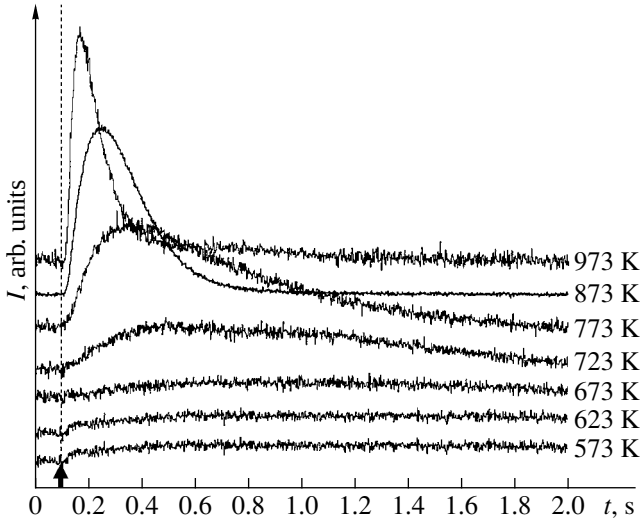

Fig. 10. O_2 profiles from Multitrack during continuous pulsing of pure N_2O over ex-FeZSM-5 at different temperatures. Cycle time, 2 s.

behavior over ex-FeZSM-5 is negligible, since the O_2 profiles obtained by pulsing N_2O only, or N_2O and NO sequentially, are very similar (not shown). It should be noted that at such high temperature N_2O conversion over the catalysts was 100% both in the absence and presence of NO under flow conditions.

DISCUSSION

As already indicated in the Introduction, the beneficial effect of NO on the activity of FeZSM-5 has been attributed by Kapteijn *et al.* [2, 3] to scavenging of adsorbed oxygen (O), regenerating the active site (Eq. (II)). The present experimental results show that scavenging of adsorbed O by NO is not the only mechanism of promotion and that NO also enhances O_2 formation. Multitrack experiments show that oxygen desorption from the catalyst surface is a relatively slow step in the reaction mechanism. In view of the slow oxygen desorption (Figs. 9, 10), the recombination of two adsorbed oxygen atoms (located on two different sites) appears the most likely explanation for O_2 formation (Eq. (VII)), rather than the reaction of N_2O with an oxidized site (Eq. (VIII)):

$$2O\square \longrightarrow O_2 + 2\square, \qquad \text{(VII)}$$

$$N_2O + O\square \longrightarrow N_2 + O_2 + \square. \qquad \text{(VIII)}$$

The dynamic nature of the adsorbed oxygen in the zeolite was studied by Valyon *et al.* [17], showing that adsorbed ^{18}O species (deposited by $N_2^{18}O$) in Fe–Mor can exchange with the lattice oxygen of the zeolite in the vicinity of Fe, so the oxygen must have a certain mobility to achieve this. The slow oxygen desorption in Fe-zeolites can then be understood by a slow migration of adsorbed oxygen atoms. This rate of desorption is higher at higher temperatures (Fig. 10) and is attributed to a higher oxygen mobility and recombination. Once adsorbed atomic O species meet each other, desorption takes place rapidly, since no O_2 adsorption was observed for FeZSM-5 [1, 18].

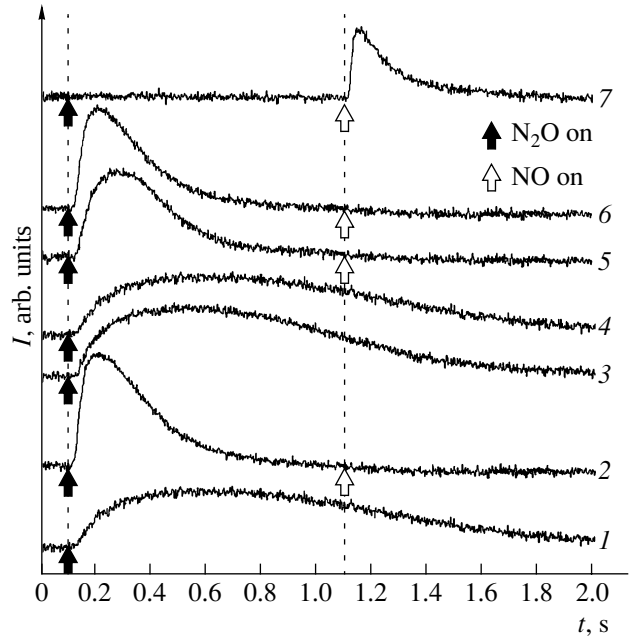

Fig. 11. O_2 profiles measured by Multitrack during catalytic decomposition of N_2O over ex-FeZSM-5 at 773 K using a cycle time of 2 s: (*1*) pulsing N_2O (at 0.1 s) and NO (at 1.1 s) after ten cycles; (*2–4*) pulsing N_2O only (at 0.1 s) two, three, and six cycles after switching off the NO valve; (*5*, *6*) pulsing N_2O (at 0.1 s) and NO (at 1.1 s) two and four cycles after switching on the NO valve, respectively; (*7*) pulsing NO.

The rate of oxygen desorption from the catalyst surface is greatly enhanced by NO addition. Indeed, a significant increase was found in the amount of oxygen formed if NO was added to the N_2O-containing feed (Fig. 11), and only a relatively small amount of NO is needed to dramatically increase the N_2O decomposition rate (Fig. 2). Although during this process NO_2 is formed, even beyond the thermodynamic equilibrium between NO, O_2, and NO_2 according to Eq. (VI) (see Fig. 3), the enhanced oxygen production strongly suggests a catalytic effect of NO. If Eq. (II) were the only promotion route induced by the addition of NO, a progressive increase in conversion upon increasing the inlet NO partial pressure would be expected. This is not the case: the promotion occurs already at relatively low substoichiometric amounts of NO, indicating the catalytic nature, and reaches a limiting value at increasing molar NO/N_2O feed ratios up to 10. This suggests the involvement of NO adsorption and that the sites where NO is adsorbed are not in competition with N_2O decomposition sites. Competitive adsorption would have resulted in inhibition, especially at high partial NO pressures. From the observation that at 698 K only four NO pulses are needed to restore the promotion effect, from the pulse size and the amount of catalyst used, and assuming that all NO adsorbed at Fe sites, it can be calculated that less than 0.9% of the Fe present is involved in the promotion. This suggests that a very low fraction of Fe is active in the reaction.

To explain the enhancement of the O_2 desorption rate at the time of the N_2O pulse, an adsorbed species formed at the time of the NO pulse needs to be involved. The amount of adsorbed NO will be reduced at high temperatures, while oxygen desorption at high temperatures already proceeds fast. This adsorption involvement is supported by the slower decay of the NO promotion at lower temperatures in the dual-pulse Multitrack experiments after NO pulsing is stopped. Sang and Lund [8] used the interconversion of nitrates and nitrites (Eqs. (IV), (V) in Introduction) to explain the enhancement of N_2O conversion by NO. However, in the infrared analysis of ex-FeZSM-5, nitrate bands have never been observed but only adsorbed NO and NO_2 species (Figs. 6, 8).

The Multitrack experiments clearly show that oxygen desorption is triggered at the time of the N_2O pulse and not at the time of the NO pulse. NO_2 formation is observed at the time of the NO pulse, indicating displacement of adsorbed NO_2 by NO as confirmed by transient *in situ* FT-IR/MS experiments. In the Multitrack formation of O_2, NO_2 is decoupled: NO_2 is mainly released due to displacement by NO and probably by thermal desorption, while O_2 is formed during the N_2O pulses. If NO_2 decomposition, as presented in Fig. 5, contributed significantly to O_2 formation, an O_2 response would have been expected at the time of the NO pulse, rather than at the time of the N_2O pulse only. This excludes the possibility that Eq. (III) is the only reason for the promotion effect.

In view of the results presented in this paper, various pathway(s) are needed to explain the catalytic effect of NO on N_2O decomposition. The different experimental observations are depicted in the scheme. The transitions of the different structures considered (A–D) are also considered in the reaction mechanism. Initially, N_2O reacts on a vacant site, yielding N_2 and leaving an oxidized site (reaction (I')). On the catalyst, a substantial amount of adsorbed NO is present, as observed by *in situ* FT-IR. Due to the absence of inhibition by NO in the activity tests and the fact that no NO signal appears at the time of the N_2O pulse in the Multitrack experiments, it is concluded that the NO adsorption and N_2O decomposition do not compete for the same site, so both processes occur at different Fe-species (light and dark solid gray areas). Adsorption of N_2O (like O□) and NO in two open coordinations at the same iron site seems hardly probable, since dinitrosyls were not identified by infrared studies in this system [O□]. As previously discussed, the production of NO_2 shown in reaction (II') is certainly not the major mode of promotion, although it cannot be completely excluded in the reaction network. In Fe-zeolite catalysts, N_2O activation occurs next to an adsorbed *NO molecule. At these temperatures (550–700 K), the oxidized site (O) subsequently oxidizes adsorbed NO to adsorbed NO_2 (reaction (III')), yielding structure C in the scheme. Subsequently, NO_2 desorption is induced by adsorption of NO (reaction (IV')), as was observed from the Multitrack experiments by the presence of a NO_2 signal at the time of the NO pulse. This closes the catalytic cycle in the conversion of N_2O and NO to N_2 and NO_2 at lower temperatures. This is in excellent agreement with the transient FT-IR/MS experiments, where NO_2 formation is observed upon switching from N_2O to NO.

Different options can be proposed to explain the enhanced oxygen formation. Again N_2O activation occurs next to an adsorbed NO molecule, yielding structure B in the scheme. Subsequently, a second N_2O molecule reacts with the site, yielding N_2 and O_2 (reaction (V')), and structure A is regenerated. The enhanced oxygen desorption from the active center has been ascribed to a reduced stability of adsorbed oxygen, induced by either electronic or steric effects of the NO adsorbed on neighboring oxidized sites. A more plausible explanation for the enhanced oxygen desorption is reaction (VI'). The increased N_2O decomposition is simply explained by the recombination of oxygen present in adsorbed NO_2 and oxygen species deposited by N_2O on a neighboring site. Alternatively, O_2 formation from NO_2, via reaction (VI'), requires competition between N_2O and NO_2 to oxidize a vacant □-site. If N_2O is a more efficient oxidizer of these sites, NO_2 levels beyond the thermodynamic equilibrium of Eq. (VI) are indeed feasible. Thus, the adsorbed NO serves to accommodate temporarily the deposited oxygen from the N_2O, freeing the neighboring site for deposition of a second oxygen. This would imply the presence of remote sites for the N_2O decomposition. Consequently,

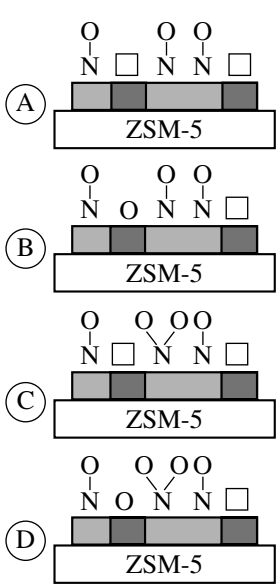

Fe-sites in the catalyst

Active Fe-sites for N_2O decomposition

No.	Elementary step			Transition
I'	$N_2O + \square$	$\longrightarrow$	$N_2 + O\square$	A $\longrightarrow$ B
II'	$NO + O\square$	$\longrightarrow$	$NO_2 + \square$	B $\longrightarrow$ A
III'	$NO_{ads} + O\square$	$\longrightarrow$	$NO_{2ads} + \square$	B $\longrightarrow$ C
IV'	$NO + NO_{2ads}$	$\longrightarrow$	$NO_2 + NO_{ads}$	C $\longrightarrow$ A
V'	$N_2O + O\square$	$\longrightarrow$	$N_2 + O_2 + \square$	B $\longrightarrow$ A
VI'	$NO_2 + O\square$	$\longrightarrow$	$NO_{ads} + O + \square$	D $\longrightarrow$ A
VII'	$NO_2 + \square$	$\longrightarrow$	$NO_{ads} + O\square$	C $\longrightarrow$ B

Scheme. Pathways in NO-assisted N_2O decomposition over ex-FeZSM-5.

the migration of oxygen atoms to recombine to molecular oxygen constitutes the rate determining process in N_2O decomposition. Taking this further, it could be speculated that the presence of NO on the catalyst surface enhances the mobility of adsorbed oxygen via an intermediate NO_2 species. This mechanism leads to faster oxygen recombination and thus to accelerated O_2 desorption. The transfer of the oxygen atom from one NO to the other is well possible, as previously observed for NO and $^{15}N^{18}O$ step changes over Cu–ZSM-5 and Cu–Y [17, 19]. Of course, O_2 formation by two adjacent adsorbed NO_2 groups cannot be ruled out.

CONCLUSIONS

NO strongly promotes N_2O decomposition over steam-activated FeZSM-5. Small amounts of NO in the feed ($NO/N_2O < 0.25$) are sufficient to produce a substantial increase in N_2O conversion for all the catalysts. Higher partial NO pressures ($NO/N_2O > 0.25$) lead to a saturation behavior of the N_2O conversion, although no inhibition by NO is observed, even at $NO/N_2O = 10$. Apparently, different sites are involved in the NO adsorption and the deposition of oxygen by N_2O. The latter sites seem to be located remotely from each other, rendering the oxygen atom recombination the rate determining process. High temperatures stimulate this process but also in the presence of adsorbed NO at lower temperatures. Adsorbed NO may temporarily accommodate oxygen deposited by N_2O on a neighboring site, allowing the deposition of a second oxygen and their recombination. Less than 0.9% of Fe seems to participate in this promotion, indicating the low density of active sites. Additionally, adsorbed NO may facilitate the migration of oxygen through NO_2 intermediates, enhancing the change of recombination to O_2.

ACKNOWLEDGMENTS

B. van der Linden and S. Mollá-Romano are gratefully acknowledged for assistance in the FT-IR/MS and the Multitrack measurements.

REFERENCES

1. Kapteijn, F., Rodríguez-Mirasol, J., and Moulijn, J.A., *Appl. Catal. B*, 1996, vol. 9, nos. 1–4, p. 25.
2. Kapteijn, F., Mul, G., Marbán, G., *et al.*, *Stud. Surf. Sci. Catal.*, 1996, vol. 101, no. 1, p. 641.
3. Kapteijn, F., Marbán, G., Rodríguez-Mirasol, J., and Moulijn, J.A., *J. Catal.*, 1997, vol. 167, no. 1, p. 256.
4. Oi, J., Obuchi, A., Bamwenda, G.R., *et al.*, *Appl. Catal. B*, 1997, vol. 12, no. 4, p. 277.
5. Centi, G., Galli, A., Montanari, B., *et al.*, *Catal. Today*, 1997, vol. 35, nos. 1–2, p. 113.
6. Pérez-Ramírez, J., Kapteijn, F., Mul, G., and Moulijn, J.A., *Chem. Commun.*, 2001, no. 8, p. 693.
7. Pérez-Ramírez, J., Kapteijn, F., Mul, G., and Moulijn, J.A., *Catal. Today*, 2002, vol. 76, no. 1, p. 55.
8. Sang, C. and Lund, C.R.F., *Catal. Lett.*, 2001, vol. 73, no. 1, p. 73.
9. Ribera, A., Arends, I.W.C.E., de Vries, S., *et al.*, *J. Catal.*, 2000, vol. 195, no. 2, p. 287.
10. Pérez-Ramírez, J., Mul, G., Kapteijn, F., *et al.*, *J. Catal.*, 2002, vol. 207, no. 1, p. 113.

11. Pérez-Ramírez, J., Berger, R.J., Mul, G., *et al.*, *Catal. Today*, 2000, vol. 60, nos. 1–2, p. 93.
12. Van Neer, F.J.R., van der Linden, B., and Bliek, A., *Catal. Today*, 1998, vol. 38, no. 7, p. 115.
13. Nijhuis, T.A., van den Broeke, L.J.P., Linders, M.J.G., *et al.*, *Catal. Today*, 1999, vol. 53, no. 2, p. 189.
14. Hadjiivanov, K., Saussey, J., Freysz, J.L., and Lavalley, J.C., *Catal. Lett.*, 1998, vol. 52, nos. 1–2, p. 103.
15. Lobree, L.J., Hwang, I.-C., Reimer, J.A., and Bell, A.T., *Catal. Lett.*, 1999, vol. 63, nos. 3–4, p. 233.
16. Lobree, L.J., Hwang, I.-C., Reimer, J.A., and Bell, A.T., *J. Catal.*, 1999, vol. 186, no. 2, p. 242.
17. Valyon, J., Millman, W.S., and Hall, W.K., *Catal. Lett.*, 1994, vol. 24, nos. 3–4, p. 215.
18. Boreskov, G.K., in *Catalysis: Science and Technology*, Anderson, J.R. and Boudart, M., Eds., Berlin: Springer-Verlag, 1982, vol. 3, p. 39.
19. Valyon, J. and Hall, W.K., *J. Catal.*, 1993, vol. 143, no. 2, p. 520.